Ann Ist Super Sanità 2012 | Vol. 48, No. 1: 19-25
DOI: 10.4415/ANN_12_01_04

Variability of morphometric parameters of human trabecular tissue from coxo-arthritis and osteoporotic samples

**Franco Marinozzi[a], Andrea Marinozzi[b], Fabiano Bini[a]
Francesca Zuppante[a], Raffaella Pecci[c] and Rossella Bedini[c]**

[a] Dipartimento di Ingegneria Meccanica e Aerospaziale, Sapienza Università di Roma, Rome, Italy
[b] Università "Campus Bio-Medico", Rome, Italy
[c] Dipartimento di Tecnologie e Salute, Istituto Superiore di Sanità, Rome, Italy

Summary. Morphometric and architectural bone parameters change in diseases such as osteoarthritis and osteoporosis. The mechanical strength of bone is primarily influenced by bone quantity and quality. Bone quality is defined by parameters such as trabecular thickness, trabecular separation, trabecular density and degree of anisotropy that describe the micro-architectural structure of bone. Recently, many studies have validated microtomography as a valuable investigative technique to assess bone morphometry, thanks to micro-CT non-destructive, non-invasive and reliability features, in comparison to traditional techniques such as histology. The aim of this study is the analysis by micro-computed tomography of six specimens, extracted from patients affected by osteoarthritis and osteoporosis, in order to observe the tridimensional structure and calculate several morphometric parameters.

Key words: microtomography, bone morphometry, osteoarthritis, osteoporosis.

Riassunto *(Variabilità dei parametri morfometrici del tessuto trabecolare umano di campioni con coxo-artrite e osteoporosi)*. I parametri morfometrici e architetturali dell'osso subiscono cambiamenti in presenza di patologie come l'osteoartrite e l'osteoporosi. Il comportamento meccanico dell'osso è influenzato sia dalla quantità (massa ossea) che dalla qualità dell'osso. La qualità dell'osso è definita da parametri che ne caratterizzano la struttura microarchitetturale, tra i principali lo spessore, la separazione e la densità trabecolare e il grado di anisotropia. Recentemente molti studiosi hanno validato la microtomografia come tecnica d'indagine della morfometria ossea e il suo notevole sviluppo è dato dal fatto che a differenza delle tecniche classiche come l'istologia, la microtomografia non provoca il danneggiamento del campione in esame. Nel corrente studio sono stati analizzati sei campioni ossei patologici tramite microtomografia computerizzata, prendendo in esame la struttura tridimensionale e i parametri istomorfometrici.

Parole chiave: microtomografia, morfometria ossea, osteoartrite, osteoporosi.

INTRODUCTION

The morphological and mechanical characterization of trabecular bone has been a widespread research topic in the last years. Trabecular bone consists of a complicated three-dimensional network of plates and rods, arranged in a lattice-like network [1]. Aging, disease process, and therapeutic agents could influence the number of elements in this network, their dimensions and connectivity, thereby causing dramatic changes in bone strength [2]. Until recently, information about structural parameters of trabecular bone were only available by histomorphometry, a destructive procedure limited to two-dimensional analysis. Micro-computed tomography (micro-CT) is an emerging technique for the non-destructive assessment and analysis of the three-dimensional trabecular bone structure. Therefore, it has been largely applied both to basic and pre-clinical bone research throughout the last several years. It relies upon the same physics principles as traditional computed tomography but has a better resolution, down to a few microns. The reconstructed image is created by irradiating the specimen with X-rays and studying the attenuation of the X-rays through the specimen, since the attenuation is directly proportional to the density of the specimen [3-5].

The mechanical strenght of bone is due to bone quantity and micro-architectural structure (quality of bone), therefore, in order to obtain a complete characterization of bone, both characteristics have

Address for correspondence: Franco Marinozzi, Dipartimento di Ingegneria Meccanica e Aerospaziale, Sapienza Università di Roma, Via Eudossiana 18, 00184 Rome, Italy. E-mail: franco.marinozzi@uniroma1.it.

to be analyzed. Microarchitecture can be assessed by several parameters: trabecular thickness (Tb. Th), trabecular number (Tb.N) and trabecular separation (Tb.Sp). Many studies underlined that these architectural parameters are related to the bone volume fraction (BV/TV) value [6-10].

The evolution of bone mass during life follows height growth. Three age-dependent phases can be distinguished: a bone mass increase until age 20, a consolidation phase, characterized by a continuous and slow increase up to age 35-40, and, finally, a progressive decrease for the rest of life. The loss of a certain amount of bone mass is physiological and unavoidable with age, and is called osteopenia. However, when this process becomes particularly intense and prolonged, enough to induce fractures or trauma, is called osteoporosis (OP).

Osteoporosis is a bone disorder characterized by an inadequate amount and faulty structure of bone, resulting in fractures from relatively minor trauma. It leads to a bone mineral density (BMD) reduction, a bone microarchitecture deterioration and an alteration of the amount and variety of proteins in bone [11, 12].

With aging, other diseases like osteoarthritis may occur. This is a metabolically active process that involves all joint tissues (cartilage, bone, synovium), mainly affecting knees, hips and small hand joints. It is caused by the breakdown and eventual loss of the cartilage of one or more joints. By aging, the water content of the cartilage increases with subsequent decrease in protein content.

In the end, cartilage begins to degenerate by flaking or forming tiny crevasses. In advanced cases, there is a total loss of cartilage cushion between the bones of the joints. Loss of the cartilage cushion causes friction between the bones, leading to pain and limitation of joint mobility can also stimulate new bone outgrowths (osteophytes) to form around the joints [13, 14].

Coxo-arthritis (CA) and osteoporosis are diseases of increasing incidence and prevalence with age [15, 16]. These pathologies and their consequent risk of fracture depend not only on the bone mass but also on the trabecular micro-architecture. The aim of this study is to evaluate some of these aspects on pathological human bone specimens using micro-CT analysis.

Because of their considerable incidence on the population, several studies have analyzed how these diseases affect bone histomorphometric parameters [17, 18].

Ding *et al.* [19], by comparing specimens of proximal tibiae from healthy donors and donors affected by osteoarthritis, demonstrated that osteoarthritic specimens show a higher BV/TV and Tb.Th and a lower bone surface to bone volume ratio (BS/BV) than control.

Fazzalari and Parkinson [20] obtained comparable results by analyzing femoral head specimens from osteoarthritic and healthy donors. Osteoarthritic specimens showed a significant decrease in Tb.N. together with an increase in Tb.Th and Tb.Sp.

Parfitt and Mathews [21] devised a new method for examining the structural changes that occur in trabecular bone by aging and in osteoporosis. Trabecular bone volume was calculated by measuring two indices, mean trabecular plate thickness (MTPT) and mean trabecular plate density (MTPD). This study confirms that osteoporotic specimens show a reduction in trabecular bone volume that is mainly due to a further reduction in plate density. Similar results were obtained by Chappard and Josselin [22] comparing twenty-four transiliac bone biopsies from patients with corticosteroid-induced osteoporosis (CSIOP) to control.

METHODS

Specimen preparation

Six trabecular bone specimens were extracted from femoral heads of three patients subjected to hip arthroplasty, affected by CA and OP.

Table 1 shows information on collected specimens such as donor sex and a brief description of pathology cases.

After identification, bone specimens were stored at -10 °C for one month then, from the frontal-plane middle-site of the femoral head, a 10 mm-thick slice was obtained for each bone specimen and stored again at -10 °C for 10 hours.

Subsequently, to defat specimens, slices were subjected to three complete cycles of dehydration with aqueous solutions with an increasing percentage of ethanol, 70%, 90% and 99.9%, respectively. Between the dehydration cycles specimens were stored at -10 °C for 10 hours.

Bone specimen slices were then cut with a diamond saw (EXTEC Labcut 1010, Enfield CT) in order to obtain 6 x 6 x 6 mm blocks, that were further dehydrated and defatted by other three cycles with ethanol solutions at different concentrations, as previously described.

Micro-CT acquisition and elaboration

Trabecular bone specimens were acquired using a Skyscan 1072 micro-CT Scanner [23]. The acquisition parameters were set at 100 kV and

Table 1 | *Characteristics (donor sex and pathologies) of examined specimens*

Specimens	Gender	Pathologies
CA1	male	medium CA
OP1	female	early OP
OP2	female	early OP
CA2	male	advanced CA with geodes
CA3	male	advanced CA with osteofytes
CA4	unknown	moderate CA

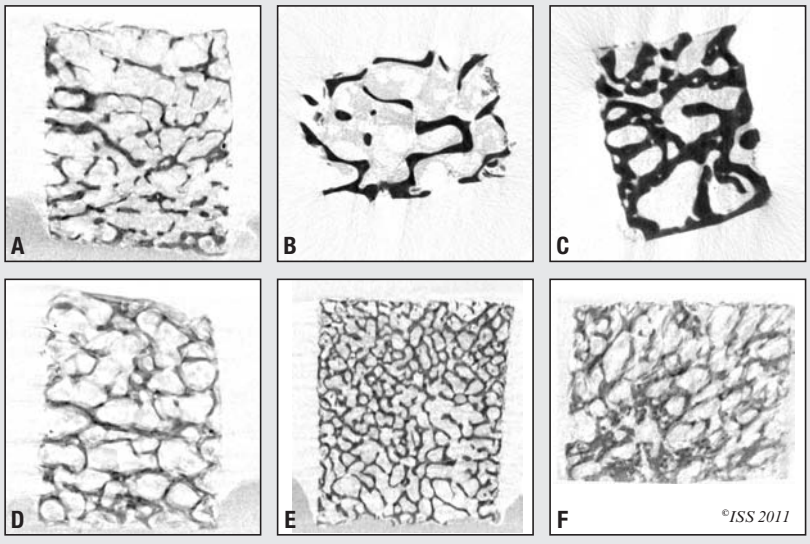

Fig. 1 | *Slice images of the specimens: (A) CA1; (B) OP1; (C) OP2; (D) CA2; (E) CA3; (F) CA4.*

98 μA, with 1 mm of aluminum filter and with a voxel size of 11.24 μm for four specimens (CA1, OP1, CA2 and CA4) and 14.66 μm for the other two (OP2 and CA3).

400 projections were acquired over an angular range of 180° by means of steps of 0.45°.

Using the cone beam reconstruction, a software based on the Feldkamp algorithm [24], projection images in TIFF format and transversal sections of the specimen in BMP format can be obtained.

Analyzing these sets of images with another software, CtAnalyser [25], the 3D structure and morphometric parameters can be processed. For this purpose, a previous process of binarization is necessary. Binarization needs to choose a threshold value that is the grey level value under which pixel is considered bone and above which pixel is considered as non-bone region. This value was selected by means of an histogram analysis, according to a previous study [26] that analyzed different methods to choose the appropriate value of threshold.

For each specimen an internal region (ROI) was selected and morphometric parameters for the corresponding volume of interest (VOI) were calculated [27]. The parameters analyzed were defined as follows:

- *bone volume/tissue volume (BV/TV, %)*, an index of bone quantity, being the percentage of the VOI occupied by bone;
- *trabecular thickness (Tb.Th, mm)* the diameter of the largest sphere which is entirely bounded within the solid surfaces;
- *trabecular separation (Tb.Sp, mm)* the thickness of the spaces as defined by binarization within the VOI;
- *trabecular number (Tb.N, 1/mm)* the number of traversals across a trabecular or solid structure made per unit length on a random linear path through the VOI;
- *trabecular thickness distribution and trabecular separation distribution* obtained by the histogram of Tb.Th and Tb.Sp calculated as a two-pixel interval.
- *degree of anisotropy* (DA) is a measure of 3D symmetry or the presence or absence of preferential alignment of structures along a particular directional axis and can assume values in the range 0 ÷ 1, where 0 values correspond to a completely isotropic structure and 1 corresponds to a completely anisotropic structure.

RESULTS

Figure 1 shows a characteristic slice for each specimen. A slice represents the transversal sections of the specimen.

The grey level histograms of the specimens obtained by processing these sets of slices are reported in *Figure 2A*. As described above, in each specimen two representative peaks of bone and air can be observed. *Figure 2B* shows the common region in which the value of grey level is constant, where analytical threshold was chosen for each specimen. Morphometric parameters and 3D structures of the specimens are shown in *Table 2* and *Figure 3*, respectively.

Differences among specimens can be firstly observed analyzing the reconstructed slices in *Figure 1* and their 3D structure in *Figure 3*, where the trabecular architecture and grey scale representation show the pathology and the withdrawal site.

The processing software allows to calculate not only the average value of Tb.Th and Tb.Sp, as reported in *Table 2*, but also the distribution of these parameters in the specimen.

Figure 4 and *Figure 5* show normalized charts of Tb.Th and Tb.Sp distribution, respectively. These charts present in x-axis the Tb.Th and Tb.Sp

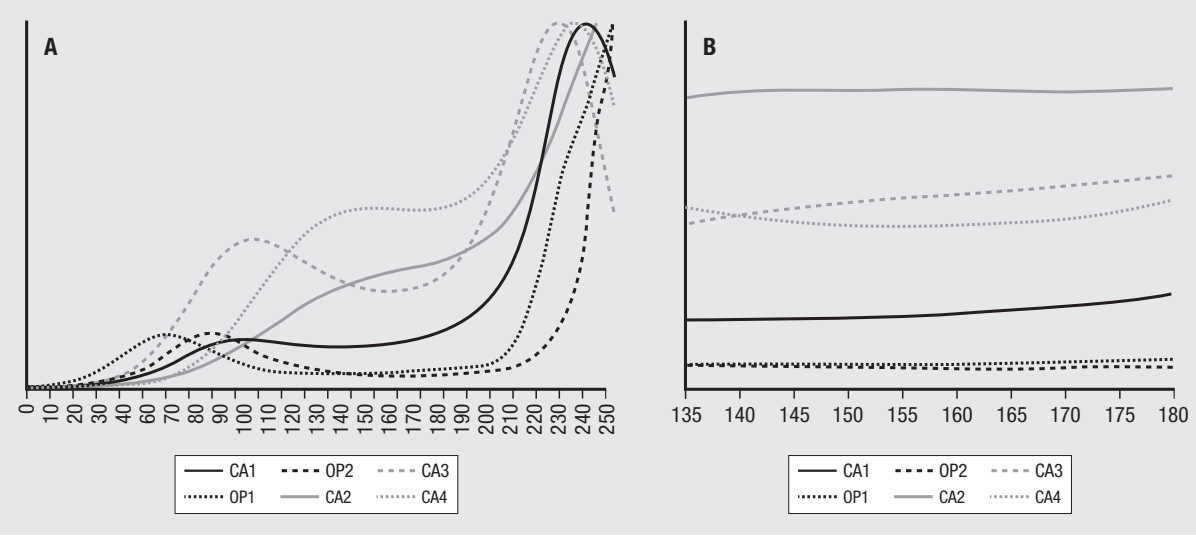

Fig. 2 | *(A) Grey level histogram of specimens; (B) Common region corresponds to the range 135÷180.*

value and in y-axis the normalized percentage of trabeculae that has the corresponding thickness and the corresponding separation.

The distributions were fitted by 6th order polynomial interpolation. Correlation coefficients between the data and the fit values are also shown *(Table 3)*. The analysis of these values is fundamental for bone characterization since they allow to obtain an accurate estimation of bone architecture.

Table 2 | *Histomorfometric parameters of the specimens*

Specimens	BV/TV (%)	Tb.Th (mm)	Tb.Sp (mm)	Tb.N (1/mm)	Degree of anisotropy
CA1	15.96	0.15	0.62	1.08	0.40
OP1	18.72	0.26	0.93	0.72	0.72
OP2	45.26	0.40	0.70	1.13	0.38
CA2	23.35	0.17	0.62	1.37	0.21
CA3	33.88	0.20	0.45	1.68	0.49
CA4	35.34	0.20	0.43	1.77	0.38

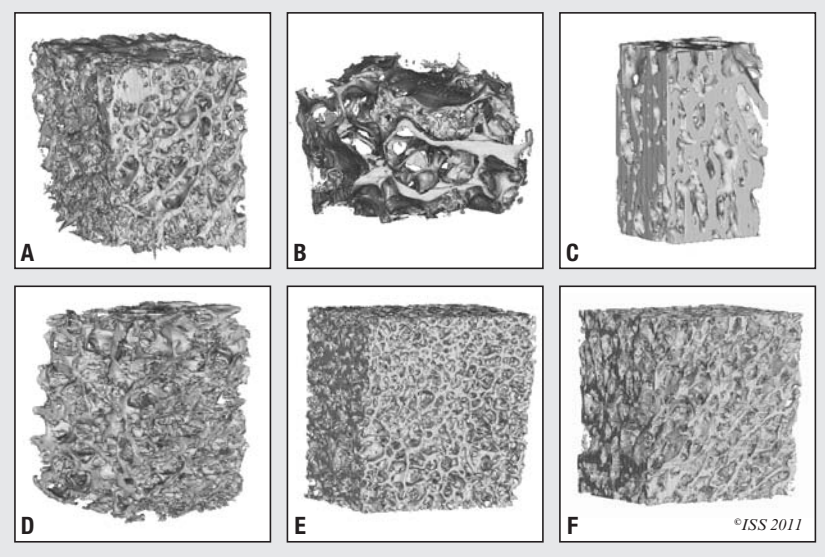

Fig. 3 | *3D structure of the specimens: (A) CA1; (B) OP1; (C) OP2; (D) CA2; (E) CA3; (F) CA4.*

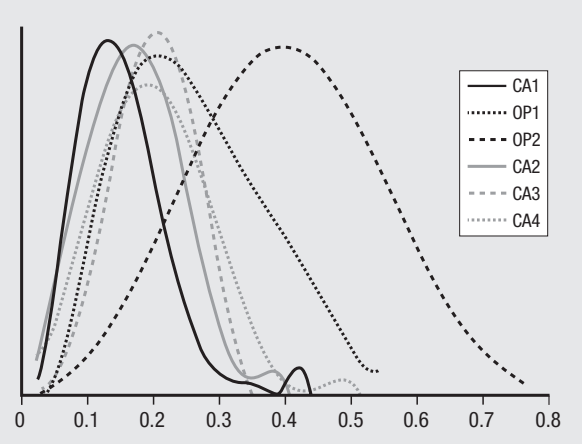

Fig. 4 | *Trabecular thickness distribution normalized and fitted by 6th order polynomial interpolation.*

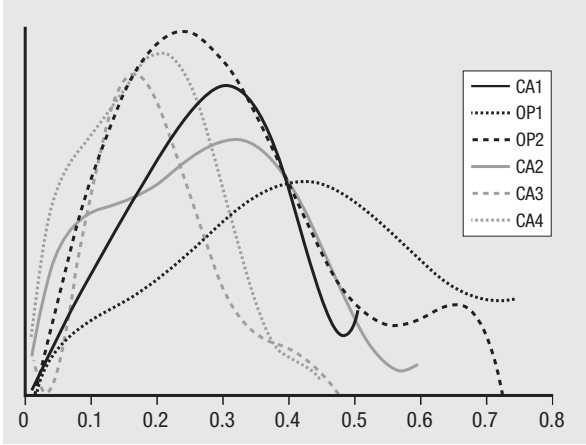

Fig. 5 | *Trabecular separation distribution fitted by 6th order polynomial interpolation.*

Moreover, these parameters undergo considerable changes in bone diseases. In particular, diseases such as osteoporosis, cause a decrease of the Tb.N and Tb.Th, and conversely an increase of the Tb.Sp value [28].

Gray levels

Since it is known that a denser material has a higher attenuation coefficient of X-rays, a grey level of an image obtained by an X-ray irradiation of a specimen can be correlated with density of the material so the grey level of each voxel represents the mineral content of the trabecular bone [29]. According to this and observing the histograms reported in *Figure 2A*, it can be observed that a peaky distribution, which could be seen for the OP specimens OP1 and OP2 and CA specimens CA3 and CA4 indicates a high trabecular tissue density. Conversely, CA1 and CA2 specimens exhibit a broader distribution around the highest grey levels and thus a lower density of the trabecular tissue.

This can also be observed in *Figure 1*, where slices of specimens characterized by a peaky distribution of grey levels present a higher difference between trabecular structure and marrow canals.

Table 3 | *Correlation coefficients between data and fits*

Specimens	R2 Tb.Th (mm)	R2 Tb.Sp (mm)
CA1	0.9721	0.9127
OP1	0.9726	0.5550
OP2	0.9788	0.9171
CA2	0.9447	0.7501
CA3	0.9734	0.9419
CA4	0.9660	0.9499

Trabecular thickness and separation

Table 2 shows that CA1 specimen has the thinnest Tb.Th population with a relatively narrow peak of 0.15 mm, CA1 also shows a relatively broad distribution with a peak value of Tb.Sp of 0.62 mm *(Figure 5)*. The Tb.N is 1.08 per millimeter, that is one of the lower value among all analyzed specimens. These morphometric parameters can explain the low value of BV/TV as compared to the other specimens.

A similar performance has been obtained as regards OP1.

OP1 specimen shows the highest value of Tb.Th and Tb.Sp, and a very broad distribution of Tb.Sp *(Figure 5)*.

A broad distribution of Tb.Th and Tb.Sp is also observed in OP2, that shows the highest value of BV/TV and also of Tb.Th *(Figure 1)*.

CA2 features a Tb.Sp rather broad distribution with two peaks.

Finally, CA3 and CA4 are characterized by similar values, and also peak distributions, of Tb.Th and Tb.Sp.

CA3 and CA4 show the highest value of Tb.N .and their high trabecular density can also be observed in *Figure 1*.

Evaluating all specimens, DA is in the range of 0.2-0.7, being CA2 the most isotropic specimen and OP1 the most anisotropic one, respectively.

CONCLUSIONS

This study shows that micro-CT is a promising technique for trabecular bone analysis. Bone morphometric parameters obtained by microtomographic processing allows to completely characterize human bone.

This analysis is also useful to compare human bone specimens with different pathologies in order to evaluate a qualitative and quantitative link be-

tween various pathologies by means of ultrastructural images and morphometric parameters.

By comparing morphometric values shown in *Table 2* with the respective gender and pathologies shown in *Table 1*, it is clear that microtomographic analysis results are in agreement with clinical data and data obtained using traditional analysis techniques [30].

The anisotropy of trabecular bone differs according to skeletal sites, and, as underlined by anatomical studies, trabecular bone femoral head is one of the highest anisotropic sites. Trabecular bone is an anisotropic material but the highest anisotropy value found in osteoporosis specimens is in accordance with the findings of Newitt *et al.* [31] who reported that the increase of bone resorption in osteoporosis leads to an increase of anisotropy.

Interestingly, in this study, Tb.Sp has obtained the highest values in the two samples of osteoporotic bone, as one might expect.

The correlation between the data obtained and the fit value has been performed in *Table 3*. High values of both parameters (Tb.Th and Tb.Sp) are evidence of the adequacy of the data obtained, with the only exception of one osteoporotic specimen.

An analysis of this kind can be helpful in *in vitro* bone studies, through diagnostic techniques, and may contribute to drug development for treatment of pathologies considered in this study.

However, to validate the promising results of this study, a considerable number of specimens should be collected and analyzed for each pathology, to gain statistical significance.

Moreover, a reliable threshold technique should be developed and applied, in order to reduce the uncertainty by which the morphometric parameters are processed.

Conflict of interest statement

There are no potential conflicts of interest or any financial or personal relationships with other people or organizations that could inappropriately bias conduct and findings of this study.

Submitted on invitation.
Accepted on 19 December 2011.

References

1. Lucy FS, William MC, Natalie S. *Bone*. Philadelphia: WB Saunders Co; 1972.
2. Gregory RM. *Anatomy, physiology and function of bone*. Michigan: The Upjohn Company; 1989.
3. Gibson LJ. Biomechanics of cellular solids. *J Biomech* 2005; 38:377-99.
4. Goldstein SA, Goulet R, McCubbrey D. Measurement and significance ofthree-dimensional architecture to the mechanical integrity of trabecular bone. *Calcif Tissue Int* 1993; 53(Suppl.1):S127-33.
5. Hildebrand T, Rüegsegger P. Quantification of bone microarchitecture with the structure model index. *Comput Methods Biomech Biomed Engin* 1997;1(1):15-23.
6. Fyhrie DP, Fazzalari NL, Goulet R, Goldstein SA. Direct calculation of the surface-to-volume ratio for human cancellous bone. *J Biomech* 1993;26:955-67.
7. Fyhrie DP, Lang SM, Hoshaw SJ, Schaffler MB, Kuo RF. Human vertebral cancellous bone surface distribution. *Bone* 1995;17:287-91.
8. Ulrich D, Hildebrand T, Van Rietbergen B, Müller R, Rüegsegger P. The quality of trabecular bone evaluated with micro-computed tomography, FEA and mechanical testing. *Stud Health Technol Inform* 1997;40:97-112.
9. Hildebrand T, Laib A, Muller R, Dequeker J, Ruegsegger P. Direct three dimensional morphometric analysis of human cancellous bone: microstructural data from spine, femur, iliac crest, and calcaneus. *J Bone Miner Res* 1999;14:1167-74.
10. Muller R, Ruegsegger P. Micro-tomographic imaging for the non-destructive evaluation of trabecular bone architecture. *Stud Health Technol Inform* 1997;40:61-79.
11. Marcus R, Majumder S. The nature of osteoporosis. In: Marcus R, Feldman D, Kelsey J (Ed.). *Osteoporosis*. 2. ed. San Diego: Academic Press; 2001. p. 3-17.
12. McNamra LM, Prendergast PJ, Schaffler MB. Bone tissue properties are altered during osteoporosis. *J Mus Neur Inter* 2005;5:342-3.
13. National Collaborating Centre for Chronic Conditions (UK). *Osteoarthritis. National clinical guideline for care and management in adults.* London: Royal College of Physicians (UK); 2008. (NICE Clinical Guidelines, No. 59).
14. Patel V, Issever AS, Burghardt A, Laib A, Ries M, Majumdar S. MicroCT evaluation of normal and osteoarthritic bone structure in human knee specimens. *J Orthop Res* 2003; 21(1):6-13.
15. Sambrook P, Naganathan V. What is the relationship between osteoarthritis and osteoporosis? *Baillieres Clin Rheumatol* 1997;11(4):695-710.
16. Cicuttini F, Wluka A, Davis S, Strauss BJ, Yeung S, Ebeling PR. Association between knee cartilage volume and bone mineral density in older adults without osteoarthritis. *Rheumatology* 2004;43(6):765-9.
17. Dougherty G. Quantitative CT in the measurement of bone quantity and bone quality for assessing osteoporosis. *Med Eng Phys* 1996;18(7):557-68.
18. Legrand E, Chappard D, Basle MF, Audran M. Evaluation of trabecular microarchitecture. Prospects for predicting the risk of osteoporosis and fracture. *Rev Rhum Engl Ed* 1999;66(11):543-7.
19. Ding M, Odgaard A, Hvid I. Changes in the three-dimensional microstructure of human tibial cancellous bone in early osteoarthritis. *J Bone Joint Surg Br* 2003;85(6):906-12.
20. Fazzalari NL, Parkinson IH. Femoral trabecular bone of osteoarthritic and normal subjects in an age and sex matched group. *Osteoarthritis Cartilage* 1998;6(6):377-82.
21. Parfitt AM, Mathews CH, Villanueva AR, Kleerekoper M, Frame B, Rao DS. Relationships between surface, volume, and thickness of iliac trabecular bone in aging and in os-

teoporosis. Implications for the microanatomic and cellular mechanisms of bone loss. *J Clin Invest* 1983;72(4):1396-409.

22. Chappard C, Peyrin F, Bonnassie A, Lemineur G, Brunet-Imbault B, Lespessailles E, Benhamou CL. Subchondral bone micro-architectural alterations in osteoarthritis: a synchrotron micro-computed tomography study. *Osteoarthritis Cartilage* 2006;14(3):215-23.
23. Skyscan. *1072 X-ray microscope instruction manual.* Aartselaar (Belgium): Skyscan Ed.; 2005.
24. Feldkamp LA, Davis LC, Kress JW. Practical cone-beam algorithm. *J Opt Soc Am A* 1984;1(6):612-9.
25. Skyscan. *CT-analyser. The user's guide.* Aartselaar (Belgium): Skyscan Ed.; 2010.
26. Bedini R, Marinozzi F, Pecci R, Angeloni L, Zuppante F, Bini F, Marinozzi A. *Analisi microtomografica del tessuto osseo trabecolare: influenza della soglia di binarizzazione sul calcolo dei parametri istomorfometrici.* Roma: Istituto Superiore di Sanità, 2010. (Rapporti ISTISAN, 10/15).
27. Parfitt AM, Drezner MK, Glorieux FH, Kanis JA, Malluche H, Meunier PJ, Ott SM, Recker RR. Bone histomorphometry: standardization of nomenclature, symbols, and units. Report of the ASBMR Histomorphometry Nomenclature Committee. *J Bone Miner Res* 1987;2(6):595-610.
28. Passariello R, Albanese C. *Osteoporosi e malattie metaboliche dell'osso: clinica e diagnostica.* Italy: Springer-Verlag; 2009.
29. Hindelang M, Maclean AL. Bone density determination of moose skeletal remains from isle Royale National Park using digital image enhancement and quantitative computed tomography. *Int J Osteoarchaeol* 1997;7(3):193-201.
30. Chappard D. Bone microarchitecture. *Bull Acad Natl Med* 2010;194(8):1469-1.
31. Newitt DC, Majumdar S, Van Rietbergen B, Von Ingersleben G, Harris ST, Genant HK, Chesnut C, Garnero P, Mc Donald B. *In vivo* assessment of architecture and micro-finite element analysis derived indices of mechanical properties of trabecular bone in the radius. *Osteoporosis Int* 2002;131:6-17.